Solar Array Mechanism Based on Deployable Structure

Shangyou Ma *

School of Civil and Resource Engineering, University of Science and Technology Beijing, Beijing, 100083, China

* Corresponding author's e-mail: 42027276@xs.ustb.edu.cn

Abstract. Spacecrafts such as satellites consume large amounts of electrical energy to carry out their missions in space. Due to the limited weight and space constraints, solar arrays become a top priority to meet the long-term operation of high-power loads. The widespread use of solar arrays is one of the necessary tools for sustainable development, which is not only related to the study of materials but also to explore more possibilities of utilization in conjunction with deployable structures. Based on the theoretical kinematic analysis and the scissor structure, this study puts forward a solar array mechanism of the scissor structure and revolute joints in the several regular polygons that connected each other. It comprises a sizeable octagonal loop and four medium-sized hexagonal rings. Because the simplified structure uses fewer rods, the failure rate is lower. A specific input angle can determine the configuration. A powerful and efficient solar array mechanism based on deployable structure was designed.

Keywords: Solar Array, Deployable Structure, theoretical kinematic, scissor structure.

1. Introduction

The field of deployable structures has experienced significant advancements in recent decades, with extensive research conducted in various aerospace applications. The primary goals of this field are to attain flexibility, large-scale capabilities, and efficient space utilization, along with dimensional expansion. So far there are many aerospace technologies have been created, for instance, space antennas [1], deployable solar arrays [2], and solar sails [3].

Spacecraft such as satellites consume large amounts of electrical energy to carry out their missions in space. Due to the limited weight and space constraints, solar arrays become a top priority to meet the long-term operation of high-power loads. With the development of spacecraft, the increase in electrical energy consumption and the higher requirements for satellite mass and space utilization has led to the development of deployable solar arrays. Figure 1. is a fully deployed square solar array.

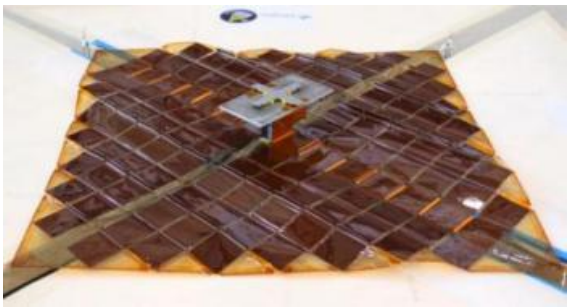

Figure 1. Fully deployed solar array. [4].

The U.S. Vanguard I spacecraft was successfully launched in March 1958, marking the first-ever utilization of solar arrays in aerospace applications. At that time, solar arrays were configured in a body-mounted arrangement, primarily used in microsatellites. Subsequent rigid unfolded solar arrays apply to most of the Earth exploration satellites. Flexible unfolded solar arrays are used on space stations and Mars landers because of their advantages of high specific power. Figure 2 shows an example of the body-mounted solar array, the rigid unfolding solar array, and the flexible unfolding solar array.

Numerous deployable structures-based solar arrays have been proposed and developed for aerospace applications, including zigzag, fan, and origami-style mechanisms. The fan mechanism

finds prominent applications in the solar arrays of satellites and landers, such as NASA's Lucy and NASA's Insight Mars Lander, as shown in Figure 3 and Figure 4, respectively. Notably, Lucy is equipped with two large circular solar cells, measuring 14.25 meters in width when unfolded, with an effective area of 51 square meters. This unique solar installation is crucial for meeting Lucy's power requirements in the challenging environment near Jupiter's Trojan belt, where sunlight intensity is less than 3% of that on Earth. Despite the weak sunlight, this solar panel can generate 500 watts of power, while Lucy's power needs are only 82 watts, ensuring ample energy for all its operations.

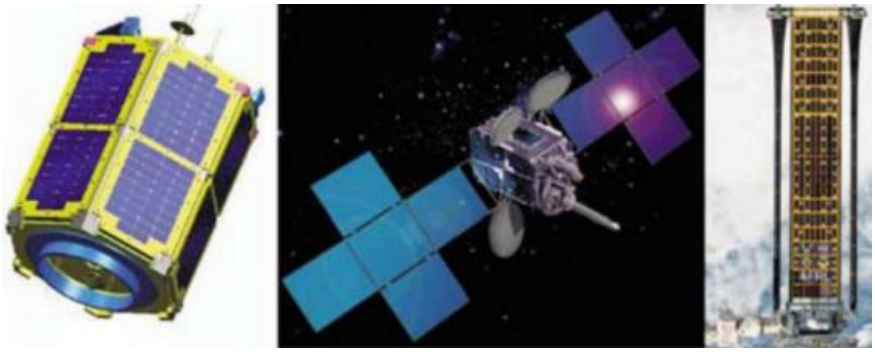

Figure 2. A body-mounted solar array, A rigid unfolding solar array, and A flexible unfolding solar array [6].

Figure 3. NASA’s Lucy [7].

Figure 4. NASA's Insight Mars Lander [8].

Motors can control the deployment of solar arrays with hinge mechanisms. Hinge mechanisms can be categorized as rigid and soft hinges [9]. The material of solar panels can be chosen as membrane structures. Membrane structures use membrane as the prime material and have a certain degree of stiffness through prestressing force or self-hardening to achieve and realize a given function. Depending on the type of support, they can be divided into air-supported and tensioned membrane structures. Considering the crease and effective area of the membrane material, the authors propose a simple unfolding structure that is easier to fabricate and connect. The deployable method by using a scissor structure to connect several approximate circular polygons is studied to support the four outer rings using retractable rods. The deployment of solar array mechanism is prevalent in constructing and power supplying for gigantic satellite institutions owing to their structural simplicity, lightweight, and innovative deployment methods that have better symmetry and stiffness. When the mechanism is subjected to bending moment due to celestial gravity and inertial forces, each part of the mechanism is stressed equally, thus ensuring stability.

In Section 2, a deployable model for the design of a solar array will be presented, along with theoretical foundation and kinematic relationships analysis. Section 3 will provide a detailed description of the deployable form of solar array mechanism, including discussions on relevant properties and kinematic relationships analysis with single input variable θ in the deploying phase. Finally, the conclusion and future work will be presented in Section 4.

2. Methods

2.1. Design and analysis of model

The author utilized the scissor structure to unfold the mechanism into a plane from a dense state by a central drive force. The conceptual design starts with analysis of the fully expanded status of the expandable structure. According to Reference [10], the author designed to use a regular octagon to be the core component. In comparison, the octagon is close to a circle than other polygons and saves more joints. The structure can be designed by adding outer ring's structure and connecting them. The structure's design determines the deployable machinery's stiffness, precision, and motion. The connection of each ring and the design of the intersection of a pair of elements with the plane also need to be considered [10].

2.1.1. Vertical view of the deployable truss

The vertical view of the deployable structure is shown in figure 5 and consists of a large loop (i.e., a positive octagonal shape) and four smaller rings (i.e., positive hexagonal shapes). The regular octagon contains one large and one small loop, each of which shares a pair of scissor elements with the other so that the four outer regular hexagonal rings can be deployed together by driving the center regular octagonal ring.

Intersection angles and points of intersection are labeled in figure 5, which will be referred to below. Based on the design of the regular octagonal inner ring, the interior angle α is angle of 45°. And the angle β of the regular hexagonal outer ring is angle of 60°.

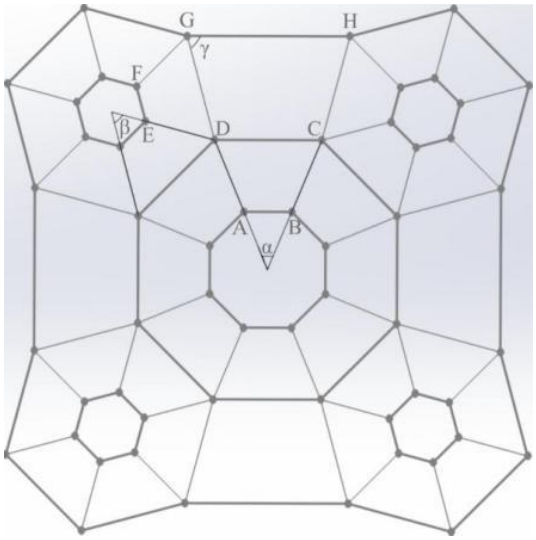

Figure 5. Vertical view of the solar array mechanism.

2.1.2. Internal, intermediate, and external connecting rods layout

Figures 6,7, and 8. respectively show the designs of the internal, intermediate that only show one side, and external connecting rods for two different kinds of links and the long-side connecting rods design of the trapezoid. Connecting rods with different lengths are marked in *a*, *b*, *c*, and *d*. Single one input variable θ is an independent variable that is a stochastic set in the deployable truss design. Meanwhile, θ is the angle between two connecting rods in each internal, intermediate, or external vertical plane. Moreover, all the intersection points of two connecting rods in these vertical planes are on the identical plane.

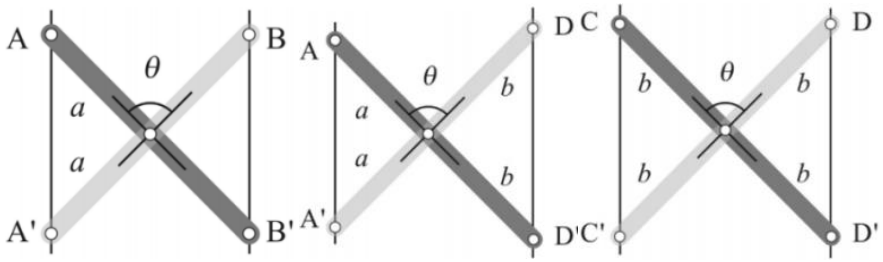

Figure 6. Internal, intermediate, and external connecting rods are designed in the link of polygon.

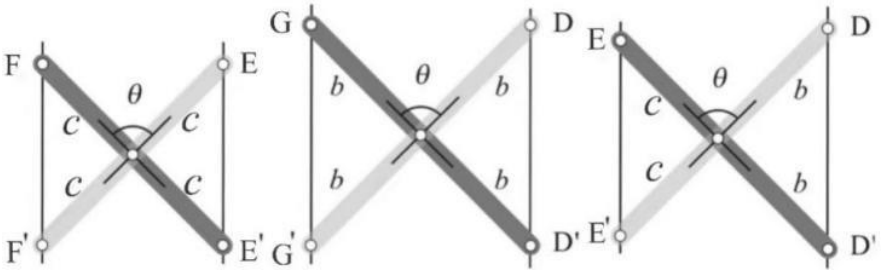

Figure 7. Internal, intermediate, and external connecting rods are designed in the link of the hexagon.

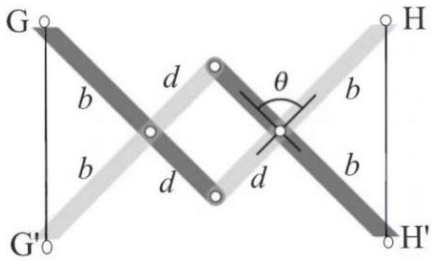

Figure 8. Border connecting rods are designed in the link of a trapezoid.

The scissor structure is crucial to the deployable mechanism. Space-developable mechanisms are multi-body systems that consist of several mechanical parts and connections, such as links and kinematic joints, which impose specific kinematic constraints or limitations on the relative motion of neighboring links [11]. Scissor constructions typically only have one degree of freedom (DOF).

However, they might have additional independent mechanism modes because of the kinematic split that occurs when they fully fold or deploy [12]. An example of a symmetric transitional scissor connection that may be entirely folded into a small bundle is one made of identical bars joined at their midpoints. As the end nodes of the bars align with the scissor hinge in this state, the linkage may become trapped. Likewise, when fully deployed, the linkage reaches its bifurcation point. In addition to the bifurcation caused by the linkage type, it can also happen because of joint clearance or bar deflection when a load is applied to the structure [13].

The bifurcation may not be preventable if the scissor structure consists of various multi-DOF scissor links. However, it might be advantageous because it enables modifying the mobility of structures with a single DOF. The deployable scissor structures are lightweight, portable, and temporary devices that can be used on a small or big scale in the architectural, engineering, and design fields [14]. The huge scale covers retractable roofs, deployable solar panels, and stages for mobile events [15]. Deployable structures have drawn increased attention in the aerospace sector due to developments in aircraft technology [16].

2.2. Kinematic Analysis

2.2.1. Theoretical Foundation

In calculating the mobility of the deployable solar array mechanism, the author simplified the motion of the spherical mechanisms and mainly analyzed the motion of the planar mechanisms that the trajectories of all pivots on its links and the axes of rotation of all revolute joints are parallel to a

plane. Figures 6 and 7 have shown that each inner ring consists of four parts of a scissor structure. Each part consists of two rigid bars(links) and five spherical pivots. Figure 8 has shown that each border connecting rod consists of four rigid bars and eight spherical pivots. The mobility of a deployable mechanism is an important aspect that can confirm the mechanism's motion if mobility is one of the scissor-like rings. Actuating central spherical pivots caused the entire mechanism to follow only one kinematic trajectory change. The ratio of each part of the rod's length according to the above Figures 5, 6, 7, and 8 also needs to be calculated.

According to Figure 5, equation (1) showed the relationship of rod's length based on the vertical view design in the regular octagon.

$$2\mathrm{AD}\sin\frac{\alpha}{2} = \mathrm{CD} - \mathrm{A}B \tag{1}$$

According to the internal, intermediate, and external connecting rods are designed in the link of the octagon in Figure 6, the length of AB, CD, and AD. can be expressed as equation (2) to equation (4), and equation (4).

$$\mathrm{AB} = 2a\sin\frac{\theta}{2} \tag{2}$$

$$\mathrm{CD} = 2b\sin\frac{\theta}{2} \tag{3}$$

$$\mathrm{AD} = (a+b)\sin\frac{\theta}{2} \tag{4}$$

Computing equation (1) to equation (4), we can get:

$$\frac{b}{a} = \frac{1+\sin\frac{\alpha}{2}}{1-\sin\frac{\alpha}{2}} \tag{5}$$

According to figure 5, equation (6) showed the relationship of rod's length based on the vertical view design in the regular hexagon.

$$2\mathrm{ED}\sin\frac{\beta}{2} = \mathrm{DG} - \mathrm{EF} \tag{6}$$

According to the internal, intermediate, and external connecting rods are designed in the link of the hexagon in figure 7, the length of EF, DG, and ED can be expressed as equation (7) to equation (9).

$$\mathrm{EF} = 2c\sin\frac{\theta}{2} \tag{7}$$

$$\mathrm{DG} = 2b\sin\frac{\theta}{2} \tag{8}$$

$$\mathrm{ED} = (b+c)\sin\frac{\theta}{2} \tag{9}$$

Computing equation (7) to equation (9), we can get:

$$\frac{b}{c} = \frac{1+\sin\frac{\beta}{2}}{1-\sin\frac{\beta}{2}} \tag{10}$$

According to Figure 5, equation (11) showed the relationship of rod's length based on the vertical view design in the trapezoid.

$$2\mathrm{GD}\sin(\frac{\pi}{2}-\gamma) = \mathrm{GH} - \mathrm{CD} \tag{11}$$

According to the internal, intermediate, and external connecting rods are designed in the link of the trapezoid in Figure 8, the length of GH can be expressed as equation (12).

$$\mathrm{GH} = 2(b+d)\sin\frac{\theta}{2} \tag{12}$$

Based on equation (8), equation (11), and equation (12), the relationship between b and d can be calculated using equation (13).

$$\frac{b}{d} = \frac{1}{2\sin(\frac{\pi}{2}-\gamma)} \tag{13}$$

The ratio of the connecting rod's length is dependent upon the layout of the ring and the angle of a, b and γ. The scissor structure allows the mechanism to fold into a compact bundle when pivoting at angle $\theta = 0$ making it ideal for applications like solar arrays that need to utilize the space effectively. For instance, in order to support the beam to carry more compressive forces, the most effective constraint against buckling is achieved for a ratio near one [10].

2.2.2. Kinematic Relationships Analysis

Solar array mechanism based on the deployable structure design is assumed to be implemented in the satellite and spacecraft. In addition, kinematic analysis of the relationship among the parameters for each component and their relations with others that only depend on a single input variable θ is also significant.

Equation (14) can be applied to compute the vertical view area of the entire mechanism. The sector area of the overall mechanism of the solar array, the central octagon loop, four hexagon rings, and four trapezoids in the border are defined as S, S_{loop}, S_{ring}, $and\ S_{trapezoid}$, respectively.

$$\begin{aligned} S &= S_{loop} + 4\times S_{ring} + 4\times S_{trapezoid} \\ &= (2+2\sqrt{2})(2b\sin\tfrac{\theta}{2})^2 + 4\times\tfrac{3\sqrt{3}}{2}(2b\sin\tfrac{\theta}{2})^2 + 4\times\frac{2b\sin\frac{\theta}{2}\cos(\frac{\pi}{2}-\gamma)[2b\sin\frac{\theta}{2}+4\sin(\frac{\pi}{2}-\gamma)+2]b\sin\frac{\theta}{2})}{2} \\ &= b^2[8+8\sqrt{2}+24\sqrt{3}+16\cos(\tfrac{\pi}{2}-\gamma)+16\sin(\tfrac{\pi}{2}-\gamma)\cos(\tfrac{\pi}{2}-\gamma)](\sin\tfrac{\theta}{2})^2 \\ &= 81.06b^2(\sin\tfrac{\theta}{2})^2 \end{aligned} \tag{14}$$

Due to the limited space available for satellites and spacecraft, it is necessary to analyze the supreme length of the entire mechanism when folded into a compact bundle, which depends on the longest bar of the peripheral ring in the regular octagon. Based on the design of the peripheral elements b shown in figure 7, the supreme length of the deployable solar array mechanism can be computed by equation (15).

$$H_b = 2b\cos\frac{\theta}{2} \tag{15}$$

Specifically, this study emphasizes how the solar array can be unfolded from a compact bundle to an astronomical plane, and the transforming of the mechanism will be analyzed below to depict the space utilization volume that the unfolding method will take up as it unfolds. In calculating this, the authors simplified the mechanism by replacing it with a combination of one octagonal prism (central loop) and four hexagonal prisms (four small rings) that transform with the single input variable expressed in equation (16).

$$\begin{aligned} V &= S\times H_b \\ &= 81.06b^2(\sin\tfrac{\theta}{2})^2\times 2b\cos\tfrac{\theta}{2} \\ &= 162.12b^3(\cos\tfrac{\theta}{2})(\sin\tfrac{\theta}{2})^2 \end{aligned} \tag{16}$$

Set the number of sides of the polygon to be n and the degree of the central angle in the different sectors to be a. The relationship between a and b is expressed by Equation (17) determined by the authors' design. Figure 9 depicts the length ratio according to equations (5) and (10).

$$\alpha = \frac{2\pi}{n} \tag{17}$$

Figure 9. showed that $n = 8$ with $\frac{b}{a} = 2.239$ and $n = 8$ with $\frac{b}{c} = 3$.

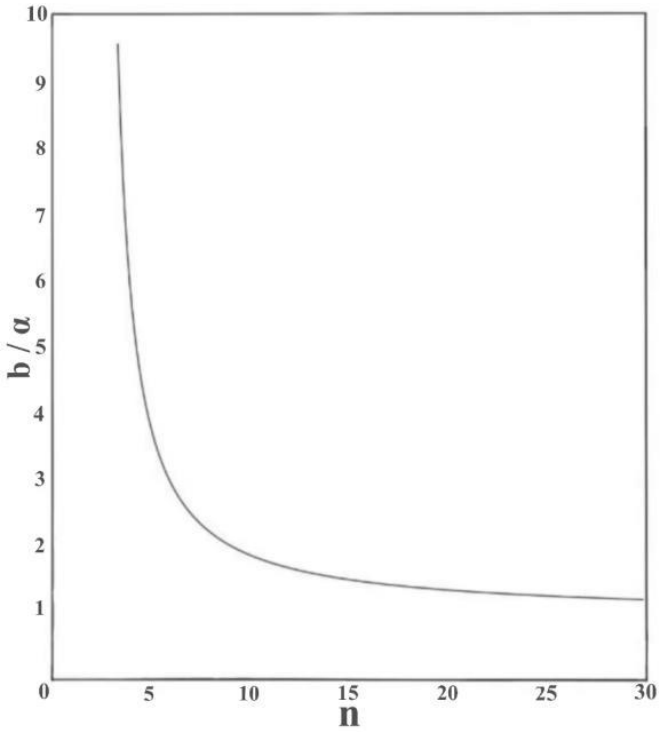

Figure 9. Relationship between the number of sides of the polygon and length ratio

3. Results

3.1. Deployable form of solar array mechanism

Figure 10. Completely folded compact bundle when pivoting at angle $\theta = 0$

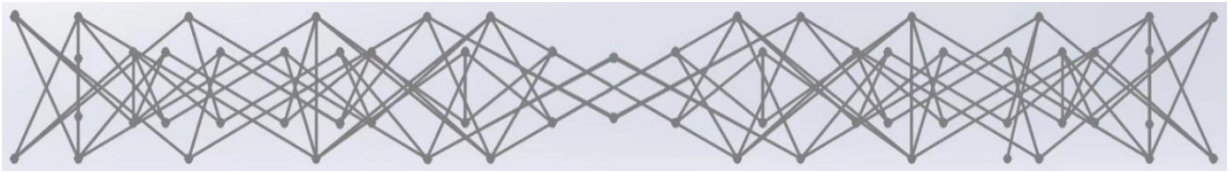

Figure 11. Side view of the whole mechanism.

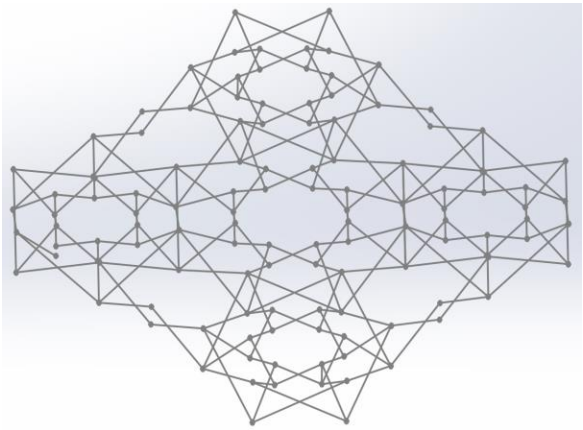

Figure 12. SolidWorks mechanism when pivoting at angle $\theta = 120^{\circ}$.

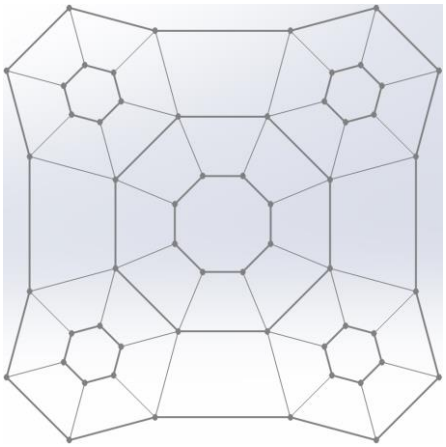

Figure 13. Completely deployable mechanism when pivoting at angle $\theta = 180^{\circ}$.

3.2. Analysis of mechanical properties

According to figure 5, the length ratios of this mechanism are *b/a* = 2.239 and *b/c* = 3. In addition, the angles are $\alpha = 45°, \beta = 60°$ and $\gamma = 70^{\circ}$. Combining equation 5 and equation 10, the design parameters $b = 2.239a, c = 0.7466a$ and $d = 1.531a$ are obtained by assuming that a is a unit length.

Based on the analysis above the solar array mechanism has only one degree of freedom and the single input variable θ is to change the central angle in the middle of each scissor structure in order to determine a configuration of the solar array mechanism. When the central angle is changed, the mechanism follows a constant trajectory.

3.3. Kinematic relationships analysis with single input variable θ

The mechanism parameters are determined at the beginning of the design. Besides, the area of vertical view is proportional to$\sin^2\frac{\theta}{2}$ in equation (14) as the central angle is varied with θ. The relationship is also depicted in figure 14. As the input variable θ is increased to around 90°, the mechanism unfolds faster and is slowest at the initial phase when it is folded and deployed.

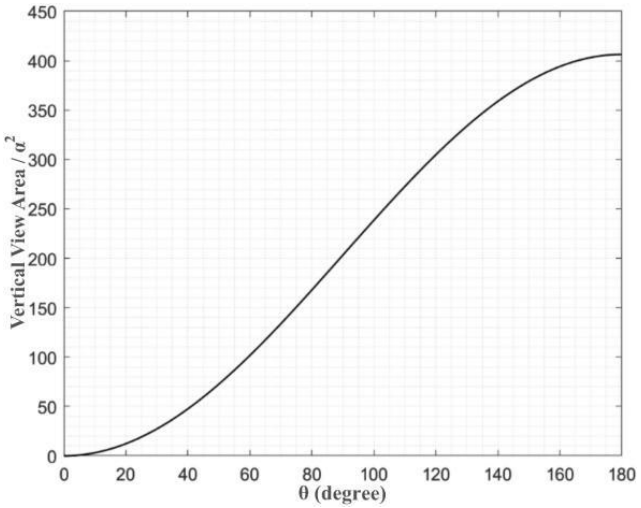

Figure 14. The vertical view area of the mechanism changing relationship with input variable θ.

The supreme length of the solar array mechanism is proportional to $\cos\frac{\theta}{2}$ in equation (15) as the supreme length is varied with θ. Figure 15 depicts that the supreme height diminishes in pivoting angle θ changed unfolding from a compact bundle to deployment to a plane. The unfolded area can be further increased to provide more energy and thus improve the spacecraft's performance.

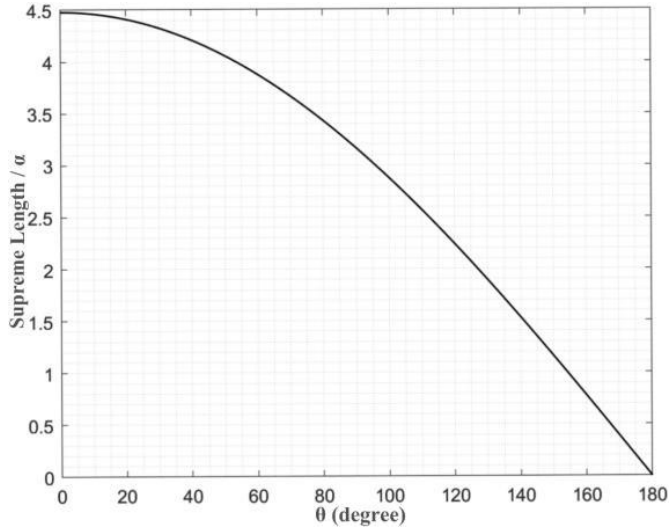

Figure 15. The supreme length of the mechanism changing relationship with the input variable θ.

The volume of the the solar array mechanism is proportional to $\sin^2\frac{\theta}{2}\cos\frac{\theta}{2}$ in equation (16) as it is varied with θ similar to a parabola. Figure 16 depicts that the maximum volume is $700.366a^3$, which occurs at $\theta = 109^{\circ}$, indicating that how much space will be occupied also needs to be noticed when the mechanism unfolds from a compact bundle to deployment to a plane.

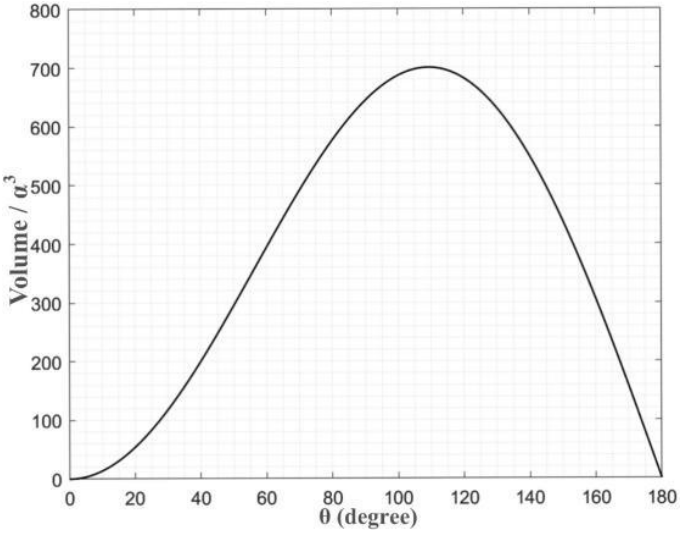

Figure 16. The volume of the mechanism changing relationship with the input variable θ.

4. Conclusion and Future Work

Based on the theoretical kinematic analysis and the scissor structure, this study puts forward a solar array mechanism of the scissor structure and revolute joints in the several regular polygons that connected each other. A powerful and efficient solar array mechanism based on deployable structure was designed. The designed structure method can solve the actual needs to complete the application by changing the value of a. For limited space and other requirements, also make the corresponding measurement criteria. This structure has only one degree of freedom due to the special feature of the scissor structure and the polygon unfolding method. The failure rate is low because few rods are used in the comparison.

In the future, combined with membrane structure and research in solar panel conversion efficiency will be more practical applications. Meanwhile, it is possible to consider increasing the number of outer rings and changing the degree of the central angle to augment the number of scissor structures to disperse the mechanical pressure more efficiently.

References

[1] You, Z. (2000) Deployable structure of curved profile for space antennas. J. Aerosp. Eng., 13.4: 139 - 143.

[2] Yuanyuan LI, Meng LI, Yufei LIU, Xinyu GENG, Chengbo CUI, Parameter optimization for torsion spring of deployable solar array system with multiple clearance joints considering rigid– flexible coupling dynamics, Chinese Journal of Aeronautics, Volume 35, Issue 3, 2022, Pages 509 - 524.

[3] Patric Seefeldt, Jan Thimo Grundmann, Martin Hillebrandt, Martin Zander, Performance analysis and mission applications of a new solar sail concept based on crossed booms with tip - deployed membranes, Advances in Space Research, Volume 67, Issue 9, 2021, Pages 2736 - 2745.

[4] F. Yves Bartsch, Patric Seefeldt, Torben Wippermann, Siebo Reershemius, Mechanical analysis of a Solar Array hinge based on a 180° folded flexible printed circuit board, Acta Astronautica, Volume 193, 2022, Pages 269 - 276.

[5] H. S. Rauschenbach, Solar cell array design handbook: the principles and technology of photovoltaic energy conversion, New York: Springer, 1976.

[6] Jiang Dongsheng, Cheng Lili. Status and future development trend of spacecraft power supply technology [J]. Power Technology, 2020, 44 (05): 785 - 790.

[7] Allison Gasparini and Lonnie Shekhtman. (2021) Watching the Blink of a Star to Size Up Asteroids for NASA's Lucy Mission. https://www.nasa.gov/feature/goddard/2021/watching-the-blink-of-a-star-to-size-up-asteroids-for-nasa-s-lucy-mission.

[8] NASA/JPL-Caltech. (2022) NASA's InSight Still Hunting Marsquakes as Power Levels Diminish https://mars.nasa.gov/news/9191/nasas-insight-still-hunting-marsquakes-as-power-levels-diminish/?site=insight.

[9] J. W. Jeong, Y. I. Yoo, J. J. Lee, J. H. Lim, and K. W. Kim, "Development of a tape spring hinge with an SMA latch for a satellite solar array deployment using the independence axiom," IERI Procedia, vol. 1, pp. 225 - 231, 2012.

[10] You, Zhong, and Yan Chen. (2012) Motion structures: deployable structural assemblies of mechanisms. Taylor & Franc.

[11] Yuanyuan Li, Yang Yang, Meng Li, Yufei Liu, Yufei, Huang, Dynamics analysis and wear prediction of rigid-flexible coupling deployable solar array system with clearance joints considering solid lubrication, Mechanical Systems, and Signal Processing, Volume 162, 2022.

[12] C.J. Gantes, Deployable Structures: Analysis and Design, WIT Press, Boston (2001).

[13] T. Buhl, F.V. Jensen, S. Pellegrino, Shape optimization of cover plates for retractable roof. structures. ComputStruct., 82 (15 – 16) (2004), pp. 1227-1236, 10.1016/j.compstruc.2004.02.021.

[14] Najmeh Faghih Dinevari, Yaser Shahbazi, Feray Maden, Geometric and analytical design of angulated scissor structures, Mechanism and Machine Theory, Volume 164, 2021, 104402, ISSN 0094 - 114X.

[15] P. A. Bernhardt, C.L. Siefring, J.F. Thomason, S.P. Rodriquez, A.C. Nicholas, S.M. Koss, M. N. urnberger, C. Hoberman, M. Davis, D.L. Hysell, M.C. Kelley, Design, and applications of a versatile H.F. radar calibration target in low Earth orbit. Radio Sci., 43 (01) (2008), pp. 1- 2310.1029/20 07RS0 03692.

[16] F. Escrig, J.P. ValcarcelGreat size umbrellas with expendable bar structures, in: Proceedings of the First International Conference on Lightweight Structures in Architecture (1986), pp. 676 - 681.